Asymmetric Photoelectron Angular Distributions from Interfering Photoionization Processes

Yi-Yian Yin, Ce Chen, and D. S. Elliott

School of Electrical Engineering, Purdue University, West Lafayette, Indiana 47907-1285

A. V. Smith

Sandia National Laboratories, Albuquerque, New Mexico 87185

We have measured asymmetric photoelectron angular distributions for atomic rubidium. Ionization is induced by a one-photon interaction with 280 nm light and by a two-photon interaction with 560 nm light. Interference between the even- and odd-parity free-electron wave functions allows us to control the direction of maximum electron flux by varying the relative phase of the two laser fields.

Interferences between different optical interactions involving the same initial and final states have attracted a great deal of attention lately. We showed previously [1] the variation of atomic excitation probability in mercury with the relative phase of the fields when a laser field and its third harmonic were focused into a mercury vapor cell. The interfering interactions have also been demonstrated in the total ionization rate in a molecular system, HCl, by Park, Lu, and Gordon [2]. We have also demonstrated the effect of phase and amplitude variations of focused beams on the interference measurements [3]. Muller *et al.* [4] exploited the interfering interactions as a probe of above threshold ionization (ATI) effects in atomic krypton using an electron detector sensitive to electrons ejected only in the direction of the laser polarization. Calculations of this interference effect for high-intensity fields have been reported [5,6]. Similar results involving one- and two-photon absorption by a photocathode were reported by Baranova *et al.* [7,8]. These authors have recently extended their technique to an atomic system [9], and report interference for two-photon versus one-photon ionization of the 4s state of atomic sodium. Second-harmonic generation in optical fibers has been attributed [10] to the asymmetry reported in this Letter as well.

In this Letter we will discuss our observations of asymmetric photoelectron angular distributions in rubidium resulting from this type of interference. To induce this asymmetry, we generate a laser field consisting of two frequencies, one an ultraviolet field capable of photoionizing the atom through the absorption of a single photon, and the second a visible field for which the absorption of two photons is required for photoionization. The frequency of the first field is precisely twice that of the second. The continuum state produced upon interaction of the atom with this field can be expressed as a coherent combination of even-parity states (εS and εD) and an odd-parity state (εP), and is, therefore, neither symmetric nor antisymmetric. In effect, it is the asymmetry of the field which leads to an asymmetric photoelectron angular distribution. Varying the relative phase and amplitude of the two field components changes the observed asymmetry of the photoelectron angular distribution. Our re-

sults clearly show that the photoelectron fluxes in opposite directions are anticorrelated. The magnitude of the asymmetry is as large as 4:1. In this Letter, we will first present a simple theory of the asymmetry based on perturbation theory, then discuss our experimental configuration, and finally present our results.

Photoelectron angular distributions are defined in terms of the projection of the laser-excited continuum state onto a plane wave in the direction **k**, the momentum vector of the photoelectron:

$$\frac{d\sigma}{d\Omega} \propto \sum_g |\langle \mathbf{k}|H|g\rangle|^2 . \tag{1}$$

In rubidium, the atomic system used in the present experiments, the ground state $|g\rangle$ is a spherically symmetric $5s\,^2S_{1/2}$ state. The rubidium is initially unaligned, so that the two magnetic sublevels, $m_s = \pm \frac{1}{2}$, are equally populated. The angular distribution is determined by averaging over the initial spin states, and summing over the spin states of the continuum electron. The angular distribution can be written in terms of the transition matrix amplitudes T_{ij}, $i,j = +$ or $-$, where i (j) represents the spin of the final- (ground-) state electron,

$$\frac{d\sigma}{d\Omega} = \frac{1}{2}\{|T_{++}|^2 + |T_{--}|^2 + |T_{+-}|^2 + |T_{-+}|^2\} . \tag{2}$$

For ionization with moderate-intensity uv light whose frequency is greater than the ionization potential (IP) of the atom, the dominant interaction is the electric dipole interaction $5s\,^2S_{1/2} \rightarrow \varepsilon^2 P$. For a linearly polarized optical field, neglecting spin-orbit effects in the continuum, the resulting transition amplitudes T_{++} and T_{--} to the continuum state $|\mathbf{k}\rangle$ are proportional to $Y_{1,0}(\Theta,\Phi)$, where Θ is the angle between the field amplitude vector **E** and the electron momentum vector **k**. Thus the angular distribution is given by $|Y_{10}(\Theta,\Phi)|^2 \sim \cos^2\Theta$. Spin-orbit coupling in the continuum leads to an additional component to this distribution, resulting in a general form

$$\frac{d\sigma}{d\Omega} = |b_1 Y_{10}(\Theta,\Phi)|^2 + |b_2 Y_{11}(\Theta,\Phi)|^2$$

$$\propto 1 + a\cos^2\Theta , \tag{3}$$

where b_1, b_2, and α are related to transition amplitudes (including phases) for the two fine-structure states in the continuum [11,12]. It can be shown that T_{++} and T_{--} are antisymmetric functions of Θ about $\Theta = 90°$, while T_{+-} and T_{-+} are symmetric. This does not have any influence on the single-photon photoelectron angular distribution since only $|T|^2$ appears in Eq. (2).

If the wavelength of the light is increased such that $IP/2 < \hbar\omega < IP$, then the absorption of two photons is required for the photoionization of the atomic rubidium. Angular momentum selection rules for atomic dipole transitions dictate that the final continuum state is a coherent combination of $|\varepsilon D\rangle$ and $|\varepsilon S\rangle$, involving transition amplitudes of the form $Y_{20}(\Theta,\Phi)$ and $Y_{21}(\Theta,\Phi)$ for the former and $Y_{00}(\Theta,\Phi)$ for the latter. The two-photon photoelectron distribution for linearly polarized light fits the form

$$\frac{d\sigma}{d\omega} = |a_1 Y_{00}(\Theta,\Phi) + c_1 Y_{20}(\Theta,\Phi)|^2 + |c_2 Y_{21}(\Theta,\Phi)|^2$$

$$\propto 1 + a_2\cos^2\Theta + a_4\cos^4\Theta. \tag{4}$$

The magnitudes of a_1, c_1, c_2, a_2, and a_4 depend upon relative cross sections to the continuum S and D states, fine-structure interaction of the εD state, and the phase shift difference between the radial matrix elements for the transition to the S and D states [13–15]. The functions T_{++} and T_{--} for two-photon ionization can be shown to be symmetric about $\Theta = 90°$, while T_{+-} and T_{-+} are antisymmetric. These symmetry relations are exactly opposite to those of the one-photon case. Again this symmetry or antisymmetry has no influence on the two-photon angular distribution.

In the case of photoionization by the bichromatic field, this symmetry becomes of extreme importance, however. Each transition amplitude T_{ij} for photoionization is the sum of two terms, one for the single-photon interaction with the uv field, and one for the two-photon interaction with the visible field. This yields an angular distribution given by the sum of the angular distributions for the one-photon and two-photon processes individually, plus an interference term which comes from the cross product of the one- and two-photon transition amplitudes. This interference term varies sinusoidally with the phase differences of the fields $\phi_1 - 2\phi_2$ (ϕ_1 and ϕ_2 are defined as the phases of the ultraviolet and visible fields, respectively), and has terms which vary as $\cos\Theta$ and $\cos^3\Theta$. In Fig. 1 we show computer simulations of the photoelectron angular distributions for various phase differences between the transition amplitudes. The relative phase is shifted by $\pi/4$ from one plot to the next. Parameters extracted from one-photon angular distributions [12], two-photon angular distributions [15], and continuum state phase differences [16–19] have been used to generate these plots. The plots in Fig. 1 show the modulation of the angular distribution over a phase variation of π. Angular distributions for the second half of the cycle are of the same
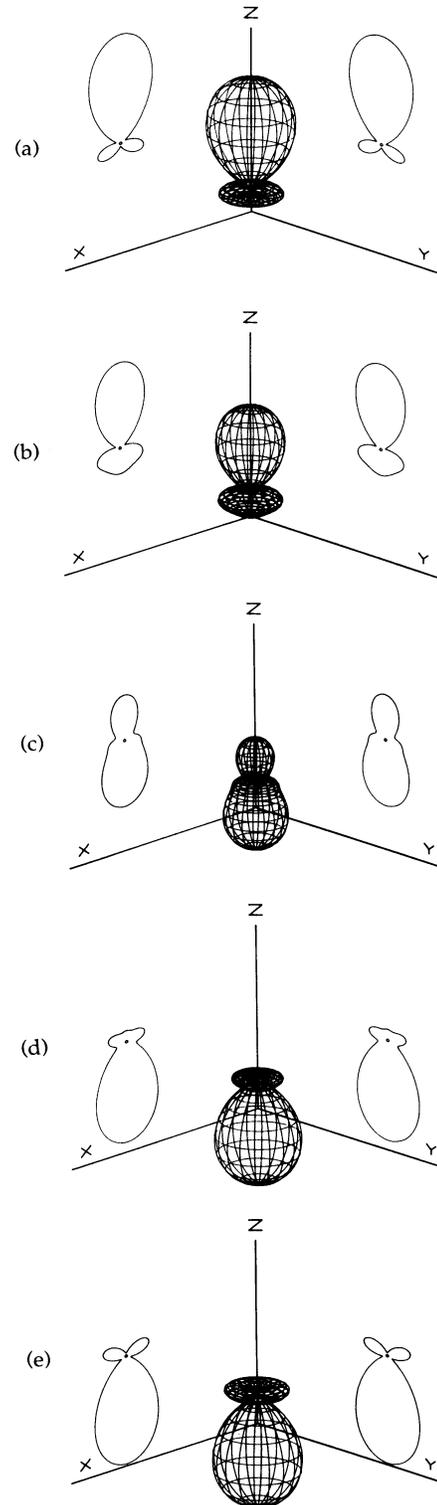
FIG. 1. Computer generated plots of the photoelectron angular distributions as a function of phase difference between the two fields. The relative cross sections for the processes are estimated from measurements of photoelectron angular distributions for one- and two-photon processes individually. The figures illustrate the angular distributions for phase increments of $\pi/4$.

form, only inverted about the origin. It is also important to note that the total cross section is not being modulated, only the angular distribution. Modulation of the total ionization rate should not be expected since the continuum states excited by the uv field and the visible field are orthogonal to each other.

The experimental configuration used to demonstrate this effect is shown in Fig. 2. A Littman-style dye laser was longitudinally pumped by the frequency-doubled output of a Q-switched Nd:YAG laser [20]. The dye laser produced 10-nsec pulses at 560 nm with a linewidth less than 5 GHz. After three stages of amplification and two spatial filters, the beam is split into two beams, each of which travels along two sides of a parallelogram before being recombined. In one branch we inserted a phase-matched frequency-doubling crystal (β-barium borate, type-I phase matching), producing an ultraviolet beam at $\lambda = 280$ nm. An absorption filter in this branch was used to block the 560-nm light. In the other branch we placed a zero-order wave plate which rotated the polarization of the 560-nm field approximately 90°, so that the polarizations of the two fields were parallel with one another. After being recombined, the two beams passed through a variable pressure gas cell, which was used to change the relative phase of the two fields, and then towards the interaction region in which the photoelectron angular distributions for the two-color photoionization of rubidium were determined.

A beam of rubidium atoms was generated in a differentially pumped high vacuum system (5×10^{-8} torr) using an effusive oven ($T \sim 160 °C$) and a pair of apertures. The density of the rubidium atoms is estimated to be 10^7 atoms cm^{-3}. The laser beams and the atom beam intersected at an angle of 108°. Four electron detectors were mounted about the interaction region in the plane nearly normal to the laser propagation direction. Each detector assembly consisted of an electron lens and a channeltron detector, and was shielded by a conducting housing. Electrons could enter the assembly only through

a 3.5-mm aperture in the shielding. Two of the detectors were aligned directly opposite each other, and were sensitive to electrons ejected along the axis of polarization of the laser beams, i.e., $\Theta = 0°$ and 180°. The other two detectors collected electrons ejected at $\Theta = 45°$ and 90°.

The pulses generated by the detectors were amplified, gated, and input to a discriminator to reduce noise. The laser pulse energy was monitored, and electron pulses were counted only for those shots whose energy was within a $\pm 5\%$ window. Electrons were counted during three data runs, each run consisting of a total of 300 acceptable laser shots for each phase setting. The data are shown in Fig. 3. The four plots report the average number of electrons per data run detected by each of the four detectors as a function of the pressure of dry N_2 in the phase delay cell. The error bars shown for a few data points indicate typical scatter among the data sets. The solid curve in each plot is the result of a fitting procedure in which the amplitude, period, offset, and phase are adjusted to minimize the mean square deviation from the data. The period of the modulation is 104 torr, in very good agreement with the predicted period of 101 torr based on refractive index dispersion data. The electron signals at 0°, 45°, and 180° show clear modulation, with the depth of modulation for the 0° and 180° signals close to 50%. This could undoubtedly be improved through better matching of the transition amplitudes for the individual interactions. The 0° and 180° signals show strong

FIG. 2. Experimental system. Elements in the diagram include the dye laser (DL), mirrors (M), beam splitter and combiner (S), BBO doubling crystal (B), uv transmitting filter (F), $\lambda/2$ retardation plate (P), and phase delay cell (DC). The polarization of the fields were as indicated. The four channel electron multiplier (CEM) detectors were positioned as shown.
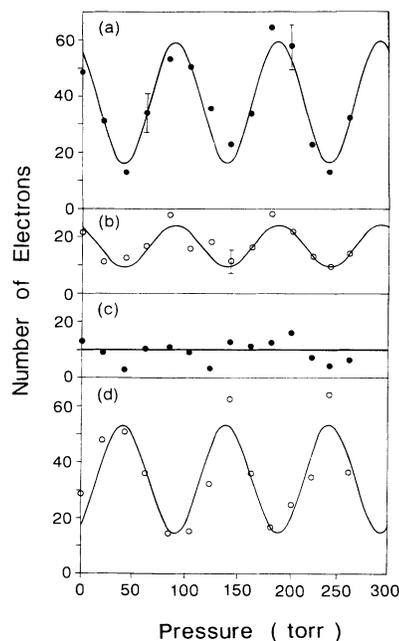
FIG. 3. Experimental data. The total electron count as a function of pressure of N_2 gas in the phase delay cell for the four detectors positioned at (a) 0°, (b) 45°, (c) 90°, and (d) 180°. The solid line is the result of a least-squares fit of a sinusoidally varying curve to the data.

anticorrelation, i.e., a 180° phase difference in the modulation. The asymmetry in the electron flux in these opposing directions is 4:1. The modulation of the 45° signal is also evident, but not as strong as that for 0° or 180°. The modulation of this signal is of nearly the same phase as the 0° signal, but the statistics are not sufficient to determine this phase shift with precision. The phase shift of the modulation for various directions Θ is expected to be dependent on the relative cross sections to the ^2S, $^2D_{5/2}$, and $^2D_{3/2}$ continuum states as well as the relative phase of these continuum state wave functions. Our theoretical analysis shows that this phase varies by almost 180° as Θ varies from 0° to 90°, with most of the variation occurring in a rather small range of Θ. The angle at which this phase variation is most rapid and the rate of change of the phase at this angle depend on these atomic parameters. Basing these determinations on measurements of phase shifts is particularly attractive since these measurements are insensitive to such factors as electron collection efficiencies or gains of the electron detectors. We plan future investigations in which we will explore the potential of using this phase shift for these determinations. The 90° signal shows no detectable modulation, in agreement with results of our analysis.

In conclusion, we have demonstrated an asymmetric distribution of the photoelectrons ejected from a spherically symmetric atom. The asymmetry can be reversed through variation of the relative phase of the two field components. In future work we will explore the potential of this phenomenon for determining accurate continuum state phase shifts, and for extending to more complex systems.

[1] C. Chen, Y.-Y. Yin, and D. S. Elliott, Phys. Rev. Lett. 64, 507 (1990).

[2] S. M. Park, S.-P. Lu, and R. J. Gordon, J. Chem. Phys. 94, 8622 (1991).

[3] C. Chen and D. S. Elliott, Phys. Rev. Lett. 65, 1737 (1990).

[4] H. G. Muller, P. H. Bucksbaum, D. W. Schumacher, and A. Zavriyev, J. Phys. B 23, 2761 (1990).

[5] K. J. Schaeffer and K. C. Kulander (to be published).

[6] R. M. Potvliege and P. H. G. Smith, J. Phys. B 24, L641 (1991).

[7] N. B. Baranova, A. N. Chudinov, and B. Ya. Zel'dovich, Opt. Commun. 79, 116 (1990).

[8] N. B. Baranova, A. N. Chudinov, A. A. Shulginov, and B. Ya. Zel'dovich, Opt. Lett. 16, 1346 (1991).

[9] N. B. Baranova, I. M. Beterov, B. Ya. Zel'dovich, I. I. Ryabtsev, A. N. Chudinov, and A. A. Shul'ginov, Pis'ma Zh. Eksp. Teor. Fiz. 55, 431 (1992) [JETP Lett. 55, 439 (1992)].

[10] See, for example, B. Ehrlich-Holl, D. M. Krol, R. H. Stolen, and H. W. K. Tom, Opt. Lett. 17, 396 (1992).

[11] T. E. H. Walker and J. T. Waber, Phys. Rev. Lett. 30, 307 (1973); J. Phys. B 6, 1165 (1973); 7, 674 (1974).

[12] Yi-Yian Yin and D. S. Elliott, Phys. Rev. A 45, 281 (1992).

[13] P. Lambropoulos and M. R. Teague, J. Phys. B 9, 587 (1976).

[14] A. Dodhy, R. N. Compton, and J. A. D. Stockdale, Phys. Rev. Lett. 54, 422 (1985).

[15] Yi-Yian Yin and D. S. Elliott (to be published).

[16] C. J. Sansonetti and K.-H. Weber, J. Opt. Soc. Am. B 2, 1385 (1985).

[17] B. P. Stoicheff and E. Weinberger, Can. J. Phys. 57, 2143 (1979).

[18] C.-J. Lorenzen and K. Niemax, Phys. Scr. 27, 300 (1983).

[19] A. Burgess and M. J. Seaton, Mon. Not. Roy. Astron. Soc. 120, 121 (1960).

[20] M. G. Littman, Appl. Opt. 23, 4465 (1984).